Chapter 3: Data Acquisition and Processing

The data acquisition includes the optical system, control software, data storage, and initial processing.

3.1 SPECTROMETER

The spectrometer used was produced by Ocean Optics, model USB-650. It has a wavelength range of 349nm to 999nm, with a resolution of 2nm (FWHM). It has 651 pixels and an adjustable integration time from 3ms to 65s.

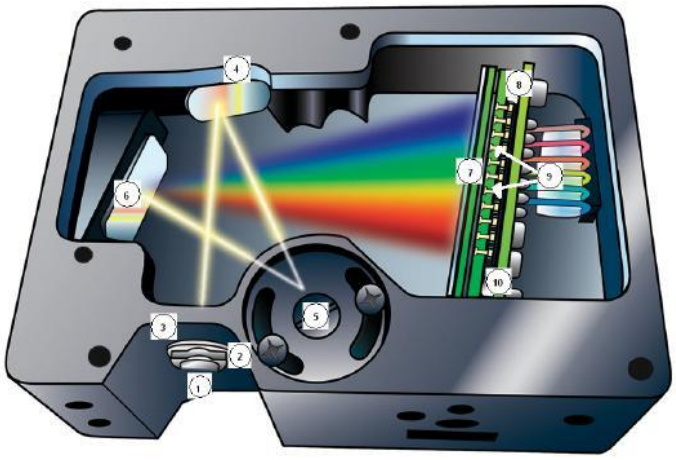

Figure 3.1: USB-650 internal view from manual [6]

The fiber optic from the collection optics connected through an SMA connection at the entrance slit, with a slit width is 25 μm.

3.2 OPTICAL SYSTEM

The Helimak plasma was viewed through an optical port on the bottom of the machine as seen in figure 3.2. The physical window was approximately 40cm wide, and gives a maximum effective viewing range of about 35cm for a 50mm lens. The lens was

mounted on a ruled linear track which also served as a position measurement. The lens was connected to the spectrometer through an optical fiber of approximately 2m in length.

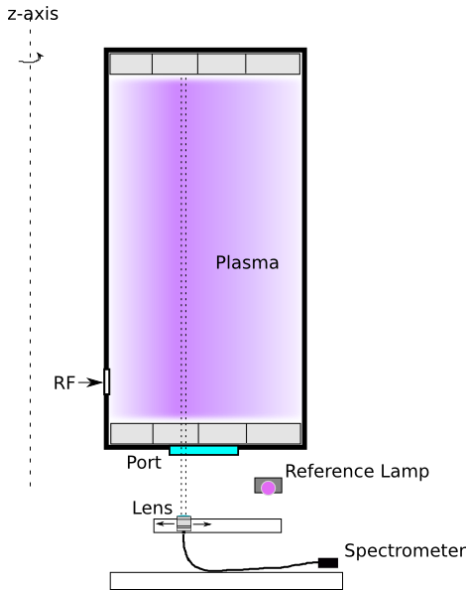

Figure 3.2: Optical system layout

The starting position of the track was measured from the inner radius of the Helimak chamber using a plumb line from the chamber to the track's position. The inner radius of the chamber was also measured to give the starting radius of the track. There were two track segments. The starting radius of the second track was also measured relative to the first track.

This allows for a measurement of only one radial position per experimental shot. The position of the lens could be changed between shots to build of a radial profile of measurements, assuming the conditions were the same for all shots.

3.3 Lens, Fiber, and Spectrometer Calibration

Calibration of the combination of the lens, fiber optic, and the spectrometer where done by taking the setup and measuring a known calibrated lamp, which was performed by William Rowan using a Lab-Sphere source at MIT. The known spectral radiance profile of the lamp $L(\lambda)$, given in units of $[\frac{W}{m^2\ sr\ nm}]$, was used to calculate a calibration constant $K(\lambda)$. A measurement of the lab-sphere emissions was made using the combination of lens, optical fiber, and spectrometer. The calibration constant was then determined using (3.1), where $N(\lambda)$ is the number of counts at a given wavelength with background subtracted, $L(\lambda)$ is the known radiance of the lamp at that wavelength, and Δt is the integration time used for the measurement. The constant can then be used to calculate the radiance of the plasma from the number of counts on the spectrometer for later measurements. The determined calibration is shown in figure 3.3.

$$K(\lambda) = \frac{N(\lambda)}{\Delta t\ L(\lambda)} \tag{3.1}$$

$$L(\lambda) = \frac{N(\lambda)}{\Delta t\ K(\lambda)} \tag{3.2}$$

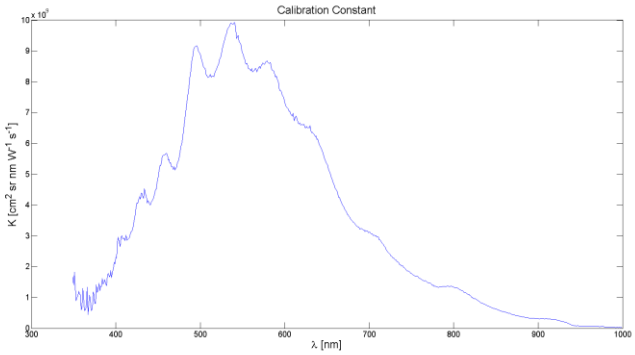

Figure 3.3: Calibration constant K versus wavelength

3.4 WINDOW CALIBRATION

The optical transmission qualities of the port window were measured as a function of position along the length of the window to account for any radial variations. The window also had a copper mesh screen on top of it to prevent RF power from escaping through the port. Calibration was accomplished by removing the entire window and screen and mounting them on a linear track. A reference light source was positioned on one side and the lens on the other, as seen in figure 3.4.

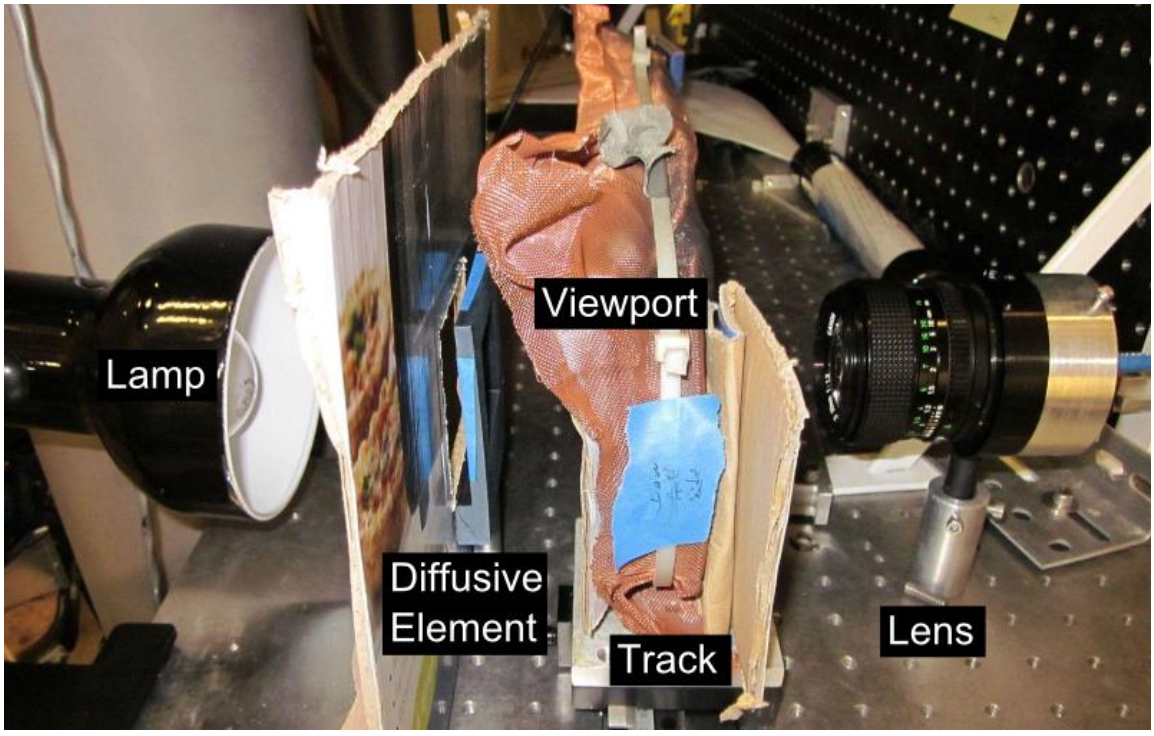

Figure 3.4: Window calibration setup

The reference light source consisted of a standard light bulb and a diffusor made a piece of paper. A measurement of the light source was made without the window in place to serve as a reference, as well as a background reference. The cardboard served to block

light to prevent the light from reflecting off of other surfaces which might contribute to the measurements.

Transmission measurements were made at 1cm increments along the length of the window. At each position, several spectra were taken and averaged together. The transmission of the window versus wavelength was calculated by dividing the measurements at each position by the measurements made without the window in place and the background subtracted. That is, the transmission is $C(\lambda, x) = I(\lambda, x)/I_0(\lambda)$. A sample of the transmission profile versus wavelength can be seen in figure 3.5 measured at position of 15cm from high field side. Figure 3.6 shows average transmission over all wavelengths versus position.

This transmission factor was included in the calibration constant for the lens/fiber/spectrometer by defining a total calibration constant in eq. 3.3.

$$K_{tot}(\lambda, x) = C(\lambda, x)K(\lambda) \tag{3.3}$$

The total calibration constant could then be used as the absolute calibration of the optical system when the lens was then aimed through the same window after it was mounted back on the Helimak. This does not, however, account for any reflections from the opposite side of the vacuum chamber as there was no proper optical dump there to prevent scattered light from entering the optics. This could cause the system to over-estimate the emission of the plasma. It was assumed that the total calibration introduces an error of around 10%.

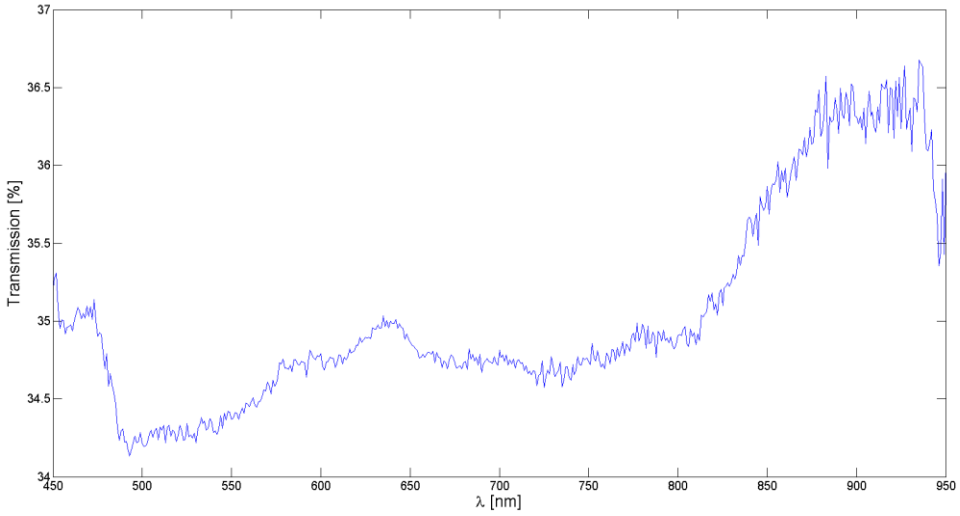

Figure 3.5: Window transmission versus wavelength at x=15cm

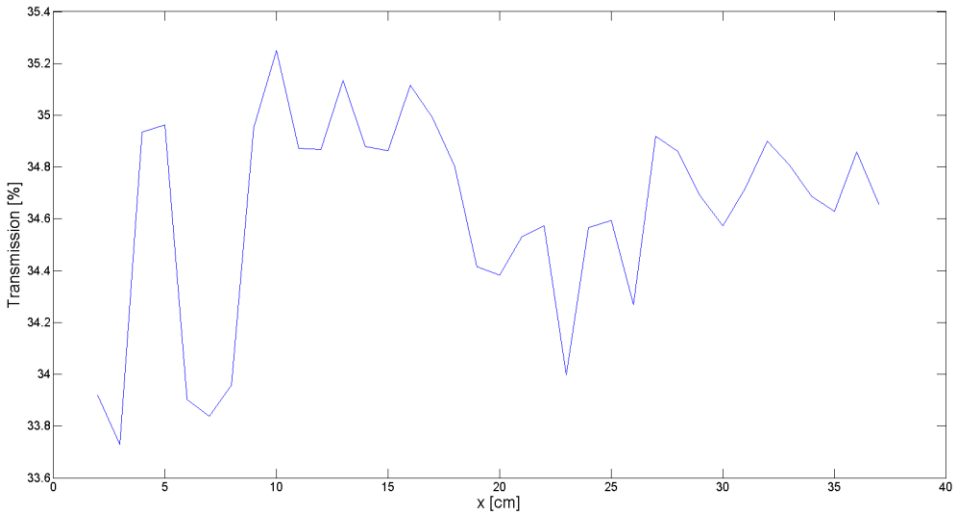

Figure 3.6: Average window transmission versus position

3.5 NEUTRAL GAS PRESSURE ACQUISITION

The neutral gas pressure was obtained from a hot filament ionization gauge which was located near the pumping system. The ionization gauge controller had a voltage output for automatic recording of the pressure. The pressure decade, in units of Torr, was given by the most significant voltage unit, and the linear scale was given by the lower significant units.

The raw voltage output was recorded by one channel of a National Instruments USB-6008 multifunction DAQ[9] as in figure 3.7. The acquisition Labview vi recorded the conversion to pressure in Torr as well as recorded the raw voltage. Only pressure readings right before each shot were taken to avoid interference from the shot itself when the data was analyzed.

Ionization gauges are typically calibrated for measuring pressure in Nitrogen, but will measure higher or lower when measuring other gases. A correction factor must be applied to the pressure reading for other gases. For Argon this factor is 1.29[7]. The actual pressure is then determined by dividing the recorded pressure by this correction factor.

Figure 3.7: USB-6008 used acquire voltage output from ionization gauge controller.

3.6 SPECTRAL ACQUISITION

A Labview vi was written to control and acquire data from the USB-650 spectrometer using the Ocean Optics Labview interface library. The control panel can be seen in figure 3.8. The vi allowed similar controls to the standard Ocean Optics control software, but also allowed customized actions.

The vi connected to the MDSPlus database of the Helimak control system, and used the MDSPlus shot event that was sent out at the beginning of each shot to automatically synchronize data acquisition with the shot. The signal was received several seconds before the shot began, which allowed acquisition during the entire shot that lasted approximately 30s.

The control panel allowed the user to set multiple integration times for the spectrometer to use during the shot. Each integration time was used in sequential order. After it had used one of each integration time it would start again with the first one. This allowed for frames with long integration times to be used for parts of the spectrum which were not as bright as other parts, while the shorter integration times were used for the intense parts of the spectrum which would saturate the detector for the longer integration times.

The control panel also had input fields for data related to the optical system, such as which lens and fiber were being used, the location and orientation of the lens during the shot, or other information that could be useful at a later date in analyzing the spectra. Once it finished acquiring the spectra during the shot, it would store the data in a human readable text file. The user would then have to set it to start waiting for the next shot.

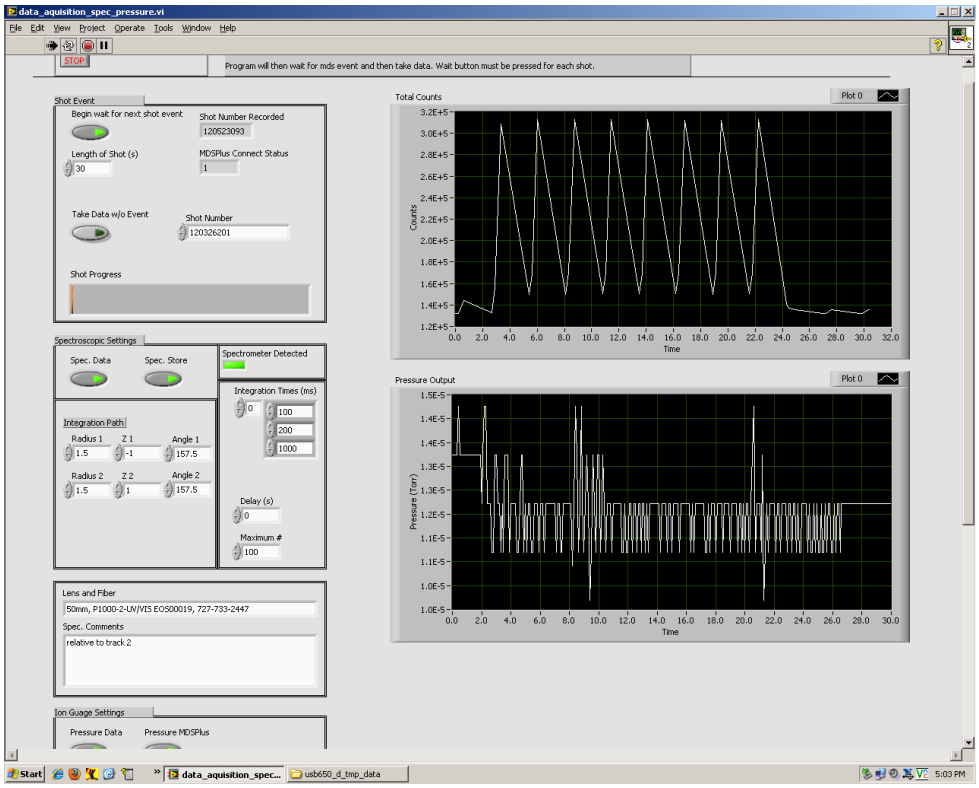

Figure 3.8: Labview acquisition control panel

In the sample screen-shot of the vi shown in figure 3.8 there are two plots shown on the right of the control panel to summarize the results at the end of each shot. The top plot shows the total number of counts from the spectrometer summed over all wavelengths versus time. The saw-tooth pattern is a result of sequentially longer and shorter integration times. Longer integrations have more counts. The start and end of plasma formation can be seen from this plot.

The bottom plot gives the recorded pressure from the ionization gauge during the shot. Some variation of the pressure reading was observed during shots, but it is not known if this is a real pressure change or if the ionization gauge was affected by the Helimak's magnetic field or some other effect during the shot.

3.7 DATA STORAGE

After each shot the vi would write the data to a data file which had a similar structure the data would have in MDSPlus. The first line of each data segment in the file contained the MDSPlus node name the data should be put into. The second line contained the data type; either numeric=0 or string=1. The third line contained the number of dimensions of the data: either 1D or 2D. If it was 1D, then the fourth line gave the number of lines of data before the next data entry and the fourth line starts listing the data. If it was 2D, then the third line gave the number of lines and the fourth line gave the number of columns.

The vi would also write to a status file which contained a number representing the status of data collection. A '0' in the file meant that collection was waiting for a shot. A '-1' in the file means data collection had ended and was not waiting for any more shots. Otherwise the number in the file was equal to the shot number from which the new data was collected. A script running in IDL would wait until the status file contained a new shot number, and would load the data from the corresponding data file into MDSPlus. The script would terminate when the status was set to '-1'.

MDSPlus does have a Labview interface which would have allowed the vi to load the data directly into MDSPlus, but the interface was found to give unpredictable results. Also, the data file acted as a human readable backup of the data.

3.8 PROCESSING RAW DATA

Before the data was used to perform analysis, initial processing was done to average all the spectra of the same integration time, apply the calibration, and convert the raw spectra into population densities of excited states for both neutral and singly ionized Argon.

Spectra were only taken into the average from the flat top operation period of each shot. There was a period of time at the beginning of each shot before which the spectra were discarded, and a period near the end after which they are discarded.

A sample spectrum with an integration time of 200ms is given in figure 3.9 after averaging over all the raw spectrum of the same integration time and subtracting the background. Figure 3.10 shows the spectrum after absolute radiance calibration is applied.

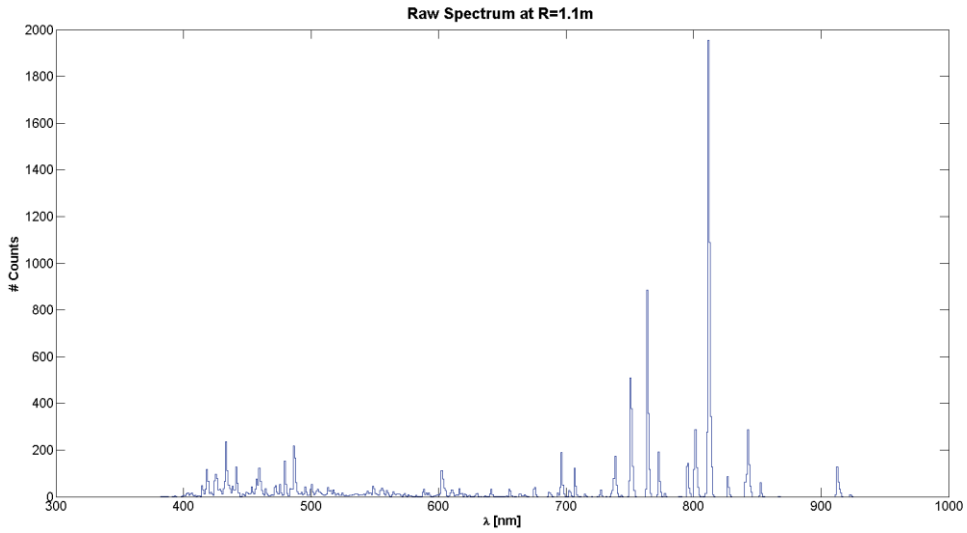

Figure 3.9: Raw spectrum at absolute radial position of 1.1m, near the peak of the temperature and density of the Helimak with an integration of 200ms.

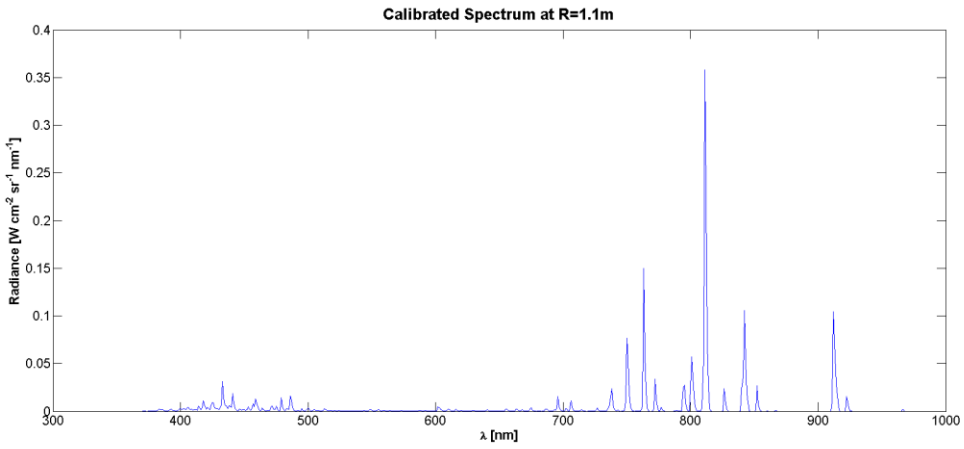

Figure 3.10: Calibration of the raw spectrum in figure 3.9 gives absolute radiance of light coming from Helimak plasma with an integration time of 200ms.

The lines below about 500nm came from singly ionized Argon, while the lines above 700nm came from neutral Argon. When the integration time of 1000ms was used as in figure 3.11, some of the dimmer lines become more defined. However, the stronger lines have saturated the spectrometer, and the values of radiance for those lines are not correct.

The next step was to convert the spectrum into population densities for the excited states of interest. Conceptually this involves integrating over a single line to get the total radiance of that line. This was implemented by using an isolated line, integrating over that line, and dividing by the peak spectral radiance of that line which gives an effective line width: $\Delta\lambda_{eff} = \int d\lambda' \, L(\lambda')/L_{peak}$. This avoids issues with overlapping lines and gives the total radiance of the line in terms of the peak value: $L_{tot} = \Delta\lambda_{eff} \, L_{peak}$ $[W \, m^{-2} \, sr^{-1}]$. The effective line width used was $\Delta\lambda_{eff} = 2.39 \, nm$.

The total radiance is related to the emission from the plasma by a chord integral representing a narrow cone from the collection lens extending through the plasma: $L_{tot} = \frac{hc}{\lambda} \int_0^l dl' \epsilon$, where ϵ is the angular photon number emission density from a single

transition in $[s^{-1}sr^{-1}cm^{-3}]$. However, since the plasma should be nearly uniform in the vertical direction, the emission density should be nearly a constant. In reality, this assumption really represents an average over the plasma: $\langle\epsilon\rangle = \frac{1}{l}\int_0^l dl'\epsilon \approx \epsilon$. The integral would then simply be the length of the chord l multiplied by the emission density. The values obtained are then sensitive to the effective chord length used. Since the plasma does not end abruptly at the termination plates, nor at the wall, the average of the two was taken to give $l = 1.72 \pm 0.28m$, where the uncertainty gives the full possible range from 1.44m up to 2m, or about 16%.

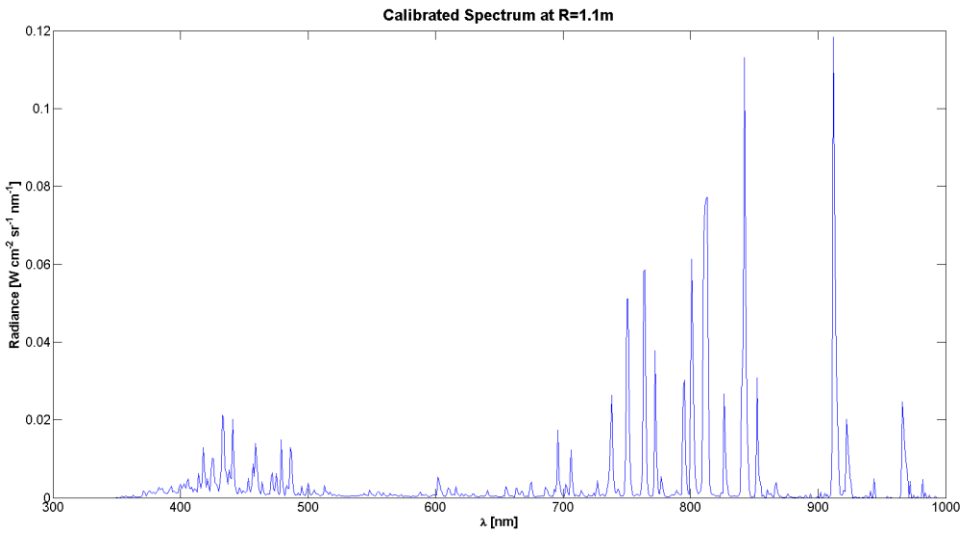

Figure 3.11: Calibrated spectrum at same radial position as figure 3.10, but with an integration time of 1000ms.

The Einstein coefficient for the transition of interest A_{ji} gives the effective frequency in $[s^{-1}]$ for the transition from excited state j to state i. It was assumed that the emission was isotropic which gave the emission density in terms of the population density of upper state j: $\epsilon = \frac{1}{4\pi}A_{ji}n_j$. Within the collisional-radiative models, the micro

states are grouped into a common state. The population density of each microstate was found in terms of the modeled state through the fractional statistical weight: $n_j = \frac{g_j}{g_k} n_k$, where $g_k = \sum g_j$ is the sum over all microstates of state k. The population density of one of the modeled excited states can then be written in terms of the absolute radiance L_{tot} as measured from the plasma and the chord integral through the plasma of length l as in eq. 3.4.

$$n_k = \frac{g_k}{g_j} \frac{4\pi}{l A_{ji}} \frac{\lambda}{hc} L_{tot} \tag{3.4}$$

3.9 Atomic Levels and Transitions

For neutral Argon, the upper state density is calculated for four of the modeled states from the Bogaerts CR model [4]. For singly ionized Argon, it is calculated for three states from the ADAS CR model.

For some upper states multiple lines are used in the determination of the density. Only those lines which do not ambiguously overlap with lines from other levels are used, which reduced the total number of available lines. If two lines from the same model level do overlap, then both are used with the coefficients from each micro-state added together. For levels that have more than one line measurement, the density is averaged between the results of the individual lines where each line is weighted equally. A total of sixteen lines are used and are tabulated in table 3.1.

line	$\lambda\ [nm]$	Ion	Upper State Term(s)	Model #	$\frac{g_j}{g_k}\frac{hc\,A_{ji}}{4\pi\lambda}\ [Wsr^{-1}]$	Δt [ms]
1	434*	Ar II	$^3P4p\ \ ^4D\ {}^3/_2 + {}^7/_2$	14	2.123e-12	1000
2	442.8*	Ar II	$^3P4p\ \ ^4D\ {}^3/_2 + {}^5/_2$	14	1.282e-12	1000
3	480.6	Ar II	$^3P4p\ \ ^4P\ {}^5/_2$	13	1.283e-12	1000
4	487.98	Ar II	$^3P4p\ \ ^2D\ {}^5/_2$	15	1.600e-12	1000
5	696.5431	Ar I	$^2P_{1/2}4p[{}^1/_2]_1$	9	1.451e-13	1000
6	706.7218	Ar I	$^2P_{1/2}4p[{}^3/_2]_2$	8	5.315e-14	1000
7	738.398	Ar I	$^2P_{1/2}4p[{}^3/_2]_2$	8	1.134e-13	1000
8	763.5106	Ar I	$^2P_{3/2}4p[{}^3/_2]_2$	7	1.268e-13	200
9	794.8176	Ar I	$^2P_{1/2}4p[{}^3/_2]_1$	8	1.388e-13	1000
10	801*	Ar I	$^2P_{3/2}4p[{}^3/_2]_2 + [{}^5/_2]_2$	7	6.999e-14	1000
11	811*	Ar I	$^2P_{3/2}4p[{}^3/_2]_1 + [{}^5/_2]_3$	7	2.990e-13	200
12	826.4522	Ar I	$^2P_{1/2}4p[{}^1/_2]_1$	9	2.928e-13	1000
13	852.1442	Ar I	$^2P_{1/2}4p[{}^3/_2]_2$	8	9.675e-14	1000
14	912.2967	Ar I	$^2P_{3/2}4p[{}^1/_2]_1$	6	3.277e-13	200
15	922.4499	Ar I	$^2P_{3/2}4p[{}^3/_2]_2$	7	2.156e-14	1000
16	965.7786	Ar I	$^2P_{3/2}4p[{}^1/_2]_1$	6	8.893e-14	1000

Table 3.1: Data used to convert the measured lines to population densities relating to the available models. One model for the Ar I levels, and one for the Ar II levels. Δt is the integration time used for each line. Wavelengths marked with * are an average of two lines.

The last step of processing of the raw data was to define a single compound excited state for both neutral and singly ionized Argon. This was done by using the statistical weights of the individual model levels to find an average density which could be divided back into the model's level densities. In this way there was a single effective excited state density used for each ion in eq. 3.5, where N=4 for ArI and N=3 for Ar II.

$$n^* = (\sum g_k)\frac{1}{N}\sum n_k/g_k \tag{3.5}$$

Ion	Model #	g_k
Ar I	6	3
Ar I	7	20
Ar I	8	8
Ar I	9	3
Ar II	13	12
Ar II	14	20
Ar II	15	10

Table 3.2: Statistical weights used for each modeled level.

The potential benefit of averaging the quantities together is to reduce the systematic error introduced by calculating the excited state densities. If the errors are random, then averaging the densities together should reduce the uncertainty by the square root of the number of lines used in the calculation. If it is assumed that each Einstein coefficient introduces an error of 10%, and each is weighted equally, then using 12 lines for Ar I would introduce an error of 3% for the calculated compound state density, and 5% for the ArII compound state from the 4 Ar II lines.

Combining with the error from calibration and the chord integral length, this gives a possible systematic error of 19% for Ar I, and 19.5% for Ar II. This does not include random errors, which can only be estimated by taking a sample of measurements. For the

example spectrum above, though, this resulted in compound excited state densities for Ar I and Ar II of $n^*_{ArI} = 2.6(5)E12\ m^{-3}$ and $n^*_{ArII} = 4.7(9)E10\ m^{-3}$.